Molecule Dynamics Simulation of Epoxy Resin System

Wu, Peilin
Department of Physics,
City University of Hong Kong.

Lam, Tran
Department of Biology,
University of Pennsylvania.

(RECSEM-2017, Joint Institute for Computational Science, University of Tennessee)
(Dated: August 4, 2017)

Glass transition and volumetric properties of a cross-linked epoxy resin system comprised of diglycidyl ether of bisphenol A and 4, 4'-Methylenebiscyclohexanamine were investigated using molecular dynamics simulations. The highly cross-linked system was constructed by activating the component molecules to simplify bond creation and allowing connections to form in a stepwise manner within a cut-off distance, equilibrating after each step. This study considered density-temperature and density-pressure relationships in cooling-down simulations. The former was used to determine the glass transition temperature (T_g), coefficient of thermal expansion α and isothermal compressibility κ. The resultant numerical values of these agree well with manufacturer ranges as well as related values for similar resins in past studies.

Keywords: molecular dynamics simulation, epoxy resin, cross-linking, volumetric properties

LIST OF FIGURES

1 BADGE (diglycidyl ether of bisphenol A) . 2
2 4, 4'-Methylenebiscyclohexanamine 2
3 Activation of amine group 3
4 Activation of epoxide group 3
5 Simulation box of $(16, 8)$ system 3
6 Simulation box of $(40, 20)$ system 3
7 Primary reaction 3
8 Secondary reaction 4
9 Schematic diagram of "bond/create" 4
10 Reaction evolution process (unwrapped) ... 4
11 Cross-linking secondary structure with 90% cross-linking percentage (unwrapped) . 4
12 Fast cooling process ($20K/500ps, T_g = 440.45K$) 5
13 Moderate cooling process ($20K/5ns, T_g = 439.36K$) 5
14 Pressurization under 300K and 500K 6

CONTENTS

List of Figures 1

Introduction 1

Simulation Methodology 2
Initial Non-cross-linked System 2
Pre-cross-linking Activation 3
Cross-linking Procedure 3
Isobaric Cooling Simulation 5
Isothermal De-pressurization Simulation 5

Results 5
Glass Transition Temperature T_g and Coefficient of Thermal Expansion α 5
Isothermal Compressibility κ 6

Acknowledgement 6

References 6

INTRODUCTION

Thermosetting epoxy resins encompass a wide range of polymeric compounds characterized by the reaction of an epoxide group-containing base resin with a curing agent (also known as a hardener) that contains reactive hydrogens. Known for their heat and electrical resistance, adhesiveness, and mechanical properties, they have been used as scratch-resistant surfaces, potting agents to reduce movement of sensitive electrical components, and adhesives in the aerospace industry, among other applications1. The desirable physical properties of epoxy resins result from the cross-linking reaction of the base resin and hardener that forms complicated, relatively rigid, and distinct microstructures[1]. Given a confluence of factors - the complex structure of epoxy resins, the relative stagnancy of development of new resin systems, and material expenses - choosing an epoxy resin for a particular application and optimizing its usage (in terms of cure temperature, cooling rate, etc.) are not trivial matters.

Relative to actual macro-scale testing that is subject to the above issues, computational approaches are attractive alternatives, able to save both time and money. In particular, molecular dynamics (MD) simulations utiliz-

ing empirically-determined parameters for atoms and potentials generated from well-documented force fields can accurately model the complicated systems at an atomistic level. As a result, several recent studies have successfully used MD simulations to model the cross-linking reaction of an epoxy resin system, with different molecular components and methodologies to resolve cross-linking formation. Wu and Xu[2] constructed a 93.7% cross-linked system by repeatedly performing energy minimization, MD simulation, and then bond formation. Both Varshney et al.[3] and Heine et al. considered a dynamic cross-linking approach where all possible reactive pairs within a cut-off were reacted simultaneously and achieved similarly high cross-linking percentages. Recently, Bandyopadhyay et al. used the LAMMPS software package to perform cross-linking on the EPON-862-DEDTA system and generated three representative systems with differing cross-linking percentages.

Irrespective of the exact procedure used to generate an initial, stable cross-linked epoxy resin system, past investigations were primarily interested in quantifying the value of physical properties relevant to practical applications. One often studied property is the glass transition temperature (T_g), the temperature below which the system is in a rigid "glassy" state and above which it is in a flexible "rubbery" state. T_g varies not only with epoxy resin composition, but also with curing conditions (like temperature) that are much easier to modify and repeat in an MD simulation than in a physical experiment. Several studies including Choi et al.[4] have found T_g values that were comparable with manufacturer-given ranges for different epoxy resins. Other physical values have been calculated as well. For example, Fan and Yuen[5] determined the system values of linear thermal expansion coefficients and Young's modulus. Wang et al.[6] and Wu and Xu[7] investigated the segmental and rotational dynamics of their cross-linked systems, finding that they significantly impacted the glass transition temperature.

This study expands upon past research computationally studying the physical properties of an epoxy resin system in multiple ways. Past studies have investigated hardeners such as TETA, IPD, and DETDA, but, to the best of our knowledge, there exists no prior work that used MD simulations to model the cross-linking of a BADGE-type base resin with a 4, 4'-Methylenebiscyclohexanamine hardener. Second, this study reports a higher degree of cross-linking in an epoxy resin system at a reasonable cut-off distance relative to earlier work. Third, in addition to quantifying temperature-related properties such as T_g and the coefficient of thermal expansion α.

SIMULATION METHODOLOGY

Initial Non-cross-linked System

The epoxy resin considered in this paper consisted of the base resin BADGE (diglycidyl ether of bisphenol A) shown in figure 1 and the amine-type hardener 4, 4'-Methylenebiscyclohexanamine shown in figure 2.

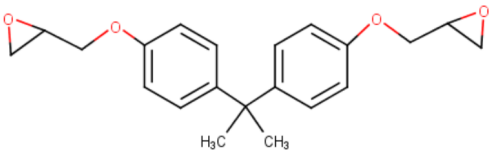

FIG. 1. BADGE (diglycidyl ether of bisphenol A)

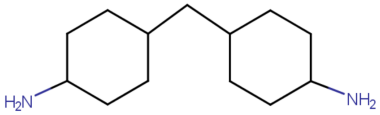

FIG. 2. 4, 4'-Methylenebiscyclohexanamine

Atom types, bonds, angles and dihedrals were parametrized under the CHARMM36[8][9] forcefield using CGenFF[10][11] and fine-tuned by analogy using VMD plugin Force Field Tookit[12]. Total potential energy under CHARMM36 forcefield is described as the summation over bonded energy and non-bonded energy terms as described below:

$$
\begin{aligned}
U_{\text{CHARMM}} = & \sum_{\text{bonds}} K_b(b-b_0)^2 \\
& + \sum_{\text{angles}} K_\theta(\theta-\theta_0)^2 \\
& + \sum_{\text{dihedrals}} K_\phi(1+\cos(n\phi-\delta)) \\
& + \sum_{\text{improper}} K_\varphi(\varphi-\varphi_0)^2 \\
& + \sum_{\text{Urey-Bradley}} K_{UB}(r_{1,3}-r_{1,3;0})^2 \\
& + \sum_{\text{CMAP}} u_{\text{CMAP}}(\Phi,\Psi) \\
& + \sum_{\text{nonb,pair}} \frac{q_i q_j}{4\pi D r_{ij}} \\
& + \sum_{\text{nonb,pair}} \varepsilon_{ij}\left[\left(\frac{R_{\min,ij}}{r_{ij}}\right)^{12} - 2\left(\frac{R_{\min,ij}}{r_{ij}}\right)^{6}\right]
\end{aligned}
$$

Structural optimization were performed using density functional theory with basis set 6-31G** [13][14] and

b3lyp[15] exchange-correlation energy[1] and the base resin and the hardener were then assigned partial charge correspond to Löwdin partial charge population analyses with NwChem[16].

Pre-cross-linking Activation

Activation approach was chosen in this study to quickly construct cross-linked structure under CHRAMM36 (which is a non-reactive force field). Assuming primary and secondary amine group are experimentally determined with approximately same reactivity as pKa values of deprotonation of both are close, all potential reactive amine groups in hardener were deprotonated as shown by figure 3.

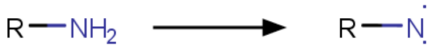

FIG. 3. Activation of amine group

Under experimental condition, epoxy resin system are placed within solutions guarantee for the hydrogen saturation of cross-linking structure. Thus, final cross-linked structures were reckoned that every epoxide group will be protonated into hydroxy group. All potential reactive epoxy groups in hardener were protonated as shown by figure 4.

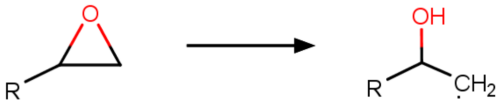

FIG. 4. Activation of epoxide group

Another series of charge population analyses and structural optimization were performed to ensure appropriate radical configuration, as activation will cause partial charge redistribution. Then, activated chemicals were packed into multiple simulation system. Then packed into a simulation box using PackMol[17][18], with an initial target density of 0.868g/cm^3 allowing larger mobility to form high percentage cross-linked structure. In diglycidyl ether of bisphenol A - 4, 4'-Methylenebiscyclohexanamine system, both radical-activated molecules are packed into simulation box with different box length with stoichiometric ration 2 : 1 denoted as (a, b) system where a, b are the number of diglycidyl ether of bisphenol A and 4, 4'-Methylenebiscyclohexanamine within the simulation box(as shown by figure 5 and figure 6).

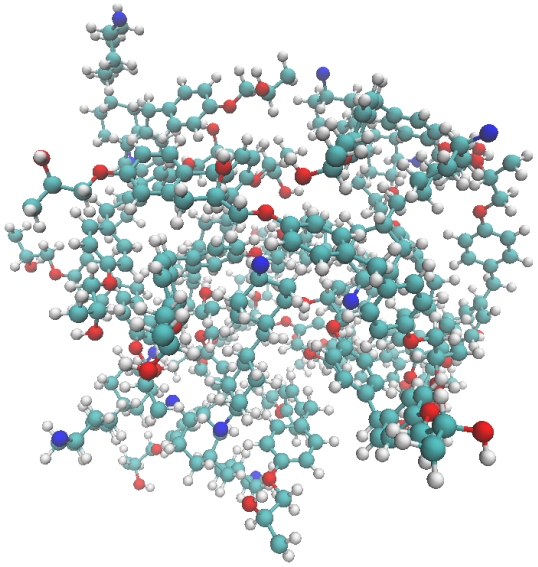

FIG. 5. Simulation box of $(16, 8)$ system

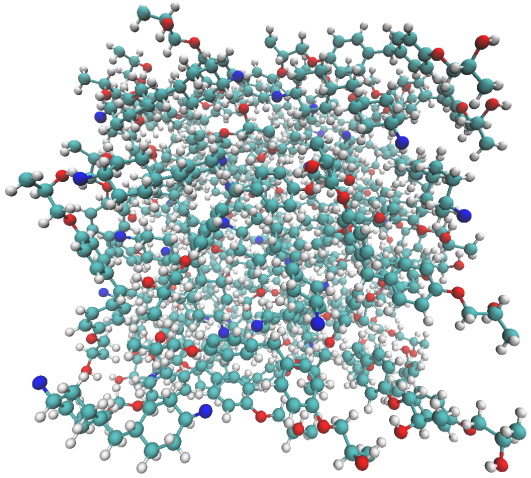

FIG. 6. Simulation box of $(40, 20)$ system

Cross-linking Procedure

The target reaction between epoxy and hardener with primary and secondary amine are shown by figure 7 and figure 8.

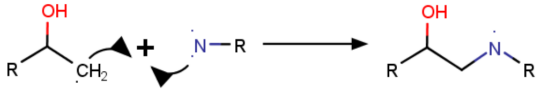

FIG. 7. Primary reaction

[1] which is computed as $E_{XC} = a_0 E_X^{HF} + (1 - a_0) E_X^{Slater} + a_X \delta E_X^{Becke88} + (1 - a_C) E_C^{VWN\perp RPA} + a_C \delta E_C^{LYP}$, where $a_0 = 0.20,\ a_X = 0.72,\ a_C = 0.81$.

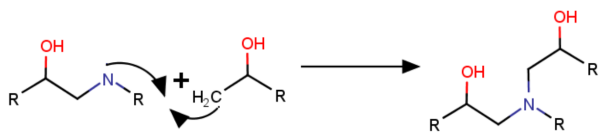

FIG. 8. Secondary reaction

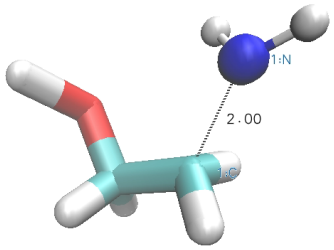

FIG. 9. Schematic diagram of "bond/create"

Cross-linking bond were formed using LAMMPS "bond/create" command under NVT ensemble with temperature 600K which allow specific bond forming between two atoms types of both are within cut-off distance as shown by figure 9. Periodic boundary condition was applied to in cross-linking formation process in order to eliminate any possible surface behaviour or other unnatural boundary structure and also to increase cross-linking percentage.

At each time step, evaluation regarding to neighbour list will conduct and connection between two atom types will be evaluated as eligible only within defined cut-off distance (in which case is 2.00Å) an then be formed with some predefined probability. Once total bond multiplicity get saturated, reactive atom will be stabilized by switching their atom types into non-reactive defined types. The large the cut-off distance, or the higher predefined probability (can be directly implies as reactivity), or the longer time range was chosen, the higher cross-linking percentage can be achieved. Cross-linking percentage was defined as:

$$\text{crosslinking percentage} = 1 - \frac{\text{noncrosslinked carbon radicals}}{\text{total potential crosslinks}}$$

Therefore, by fine-tuning cut-off distance, probability, time range, multiple snapshot of each system with different degree of propagation along reaction coordinate as defined by cross-linking percentage as shown in figure 10, as new forming cross-linking bonds were highlighted in red.

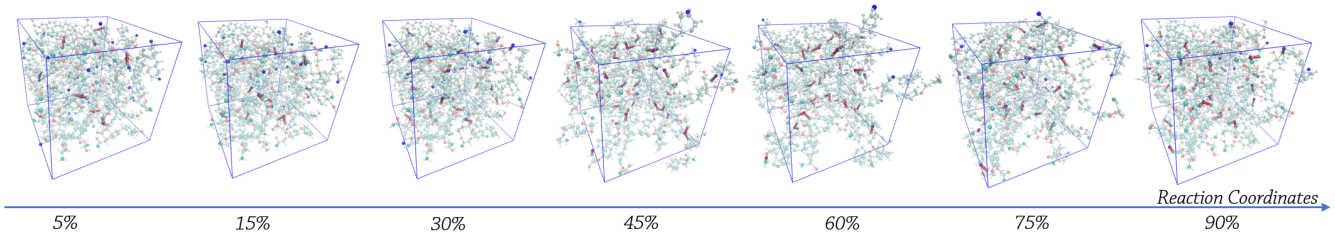

FIG. 10. Reaction evolution process (unwrapped)

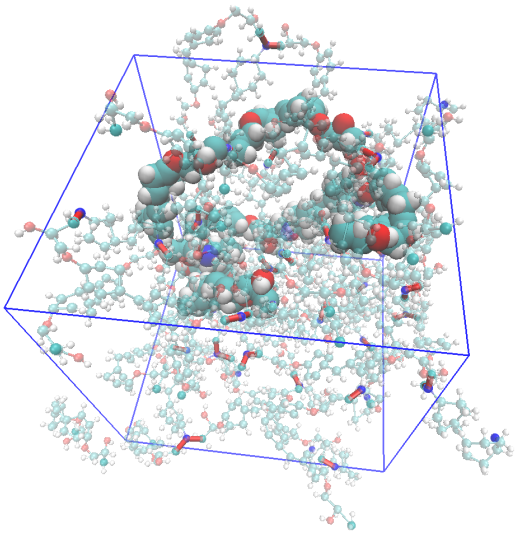

FIG. 11. Cross-linking secondary structure with 90% cross-linking percentage (unwrapped)

System with different cross-linking percentage presents different chain formation process contributing to complex secondary structures as shown by figure 11. Periodic boundary allows circular polymer chain network to be formed throughout process. The final cross-linked epoxy resin system are assumed to be protonated under experimental condition which guarantee for the hydrogen saturation, thus every remained carbon and nitrogen radical were restored and properly assigned partial charge according to previous Löwdin partial charge population analyses. Energy minimization was then performed on this system in LAMMPS with an energy stopping tolerance $1e-4$, a force stopping tolerance of $1e-6$, and a maximum of $10,000$ minimizing iterations and force/energy evaluations. This optimized configuration was then subject to the cross-linking process described

below.

Isobaric Cooling Simulation

Both stepwise cooling and heating MD simulations (for additional validation of calculated T_g) were performed on the crosslinked epoxy resin system to model the glass transition process and quantify T_g. In order to model the glass transition process and quantify T_g, this study considered both stepwise cooling (used in Wang et al.[6]). We hypothesize that the two simulations will return similar ranges for T_g, thus improving the validity of the quantification.

Two cooling simulation with different cooling rates were conducted respect to high cross-linking epoxy resin system (with 98.75% cross-linking percentage) in this study. In the rapid cooling simulation, the model was first heated to 600K and then subjected to 500ps of NVT (constant volume and temperature ensemble) equilibration and 500ps of NPT (constant pressure and temperature ensemble) at pre-clooling temperature, similar to the procedure of Wang et al.[6]. The former NVT ensemble stabilized the epoxy resin to the heightened temperature, while the latter NPT ensemble stabilized the density of the system. The system was then cooled from 600K to 300K at a rate of 20K/500ps in stepwise manner. After each 20K decrease in temperature, 500ps of NVT and 1atm NPT MD simulation was performed to allow the simulation box to expand or contract as necessary. The value of the system's volume was averaged over the last 100ps of the equilibration and taken as a data point for linear regression. The configuration after the equilibration was then taken as the initial state for cooling to the next temperature, and this process was repeated until the system cooled to 300K.

In the moderate cooling simulation, the model was first similarly heated to 600K and then subjected to 1ns of NVT equilibration and 1ns of NPT at pre-cooling temperature, and was then cooled from 600K to 300K at a rate of 20K/5ns in stepwise manner. After each 20K decrease in temperature, 5ns of NVT and 1atm NPT MD simulation was performed similarly. The value of the system's volume was averaged over the last 1ns of the equilibration and also taken as a data point for linear regression. The configuration after the equilibration was then taken as the initial state for cooling to the next temperature, and this process was repeated until the system cooled to 300K.

Isothermal De-pressurization Simulation

To determine isothermal compressibility κ, isothermal de-pressurization process was preformed to cross-linked epoxy resin system. Instead of varying over a range of temperatures to determine T_g and the coefficient of thermal expansion, quantifying isothermal compressibility requires variation over a range of pressures. A stepwise depressurization MD simulation was thus performed to model the volumetric change of the system. The pressure of the initial crosslinked system was first equilibrate to 1atm under the NPT ensemble for 25ns to stabilize the system. And then pressurization was preformed at the rate of $010atm/1ns$ in different temperatures as 500K higher than the previous determined T_g and 300K lower than T_g in a stepwise manner. The value of the system's volume was averaged over the last 2ns of the equilibration in each step and also taken as a data point for linear regression.

RESULTS

Glass Transition Temperature T_g and Coefficient of Thermal Expansion α

Glass transition temperature T_g can be determined in both fast cooling simulationand moderate cooling simulation as shown by the following figure 12 and 13:

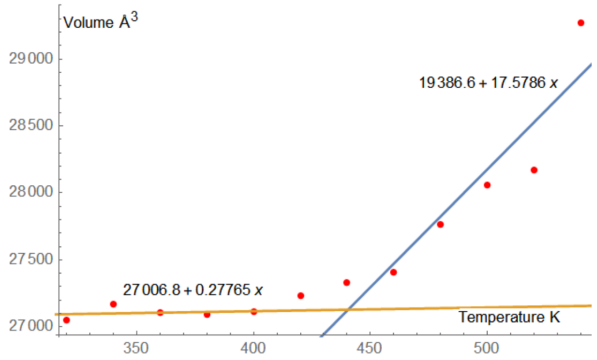

FIG. 12. Fast cooling process ($20K/500ps, T_g = 440.45K$)

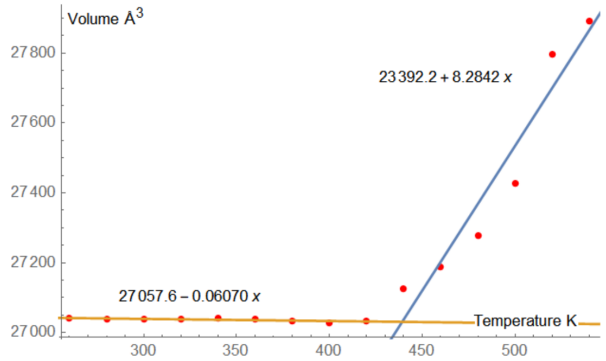

FIG. 13. Moderate cooling process ($20K/5ns, T_g = 439.36K$)

As shown in the results, this high cross-linked epoxy

resin has glass transition temperature T_g approximately equals 440K. Additionally, coefficient of thermal expansion α can also be calculated as

$$\alpha(P,\varepsilon) = \frac{1}{V}\left(\frac{\partial V}{\partial T}\right)_{P,\varepsilon} \approx \frac{1}{V}\left(\frac{\Delta V}{\Delta T}\right)_{P,\varepsilon}$$

when increment Δ are small. Thus the slope of these lines carries physical representation of coefficient of thermal expansion α. Thus for the rapid cooling process, the coefficient of thermal expansion was determined as $\alpha_{rapid,glassy} = 9.38 \times 10^{-6} K^{-1}$ which insignificant suggesting that in the glassy state, changes in temperature do not affect the system's volume to a significant extent, and $\alpha_{rapid,rubbery} = 5.10 \times 10^{-4} K^{-1}$ which is significant at the 1% level. This means in this state, the volume increases by 5 parts per 10000 per 1 Kelvin increase. While in the moderate cooling process $\alpha_{moderate,glassy} = -2.051 \times 10^{-6} K^{-1}$ which is again not significant at 1% level, while in the rubbery state $\alpha_{moderate,rubeery} = 2.51 \times 10^{-4} K^{-1}$ which is significant at the 1% level.

Isothermal Compressibility κ

As expectation, the pressurization test shows different slopes suggests different isothermal compressibility κ under different states.

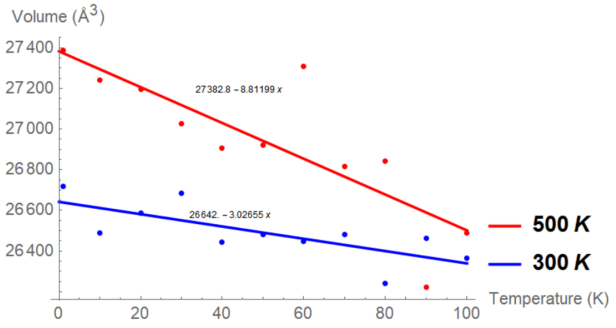

FIG. 14. Pressurization under 300K and 500K

Similarly, isothermal compressibility can be determined through

$$\kappa(T,\varepsilon) = -\frac{1}{V}\left(\frac{\partial V}{\partial P}\right)_{T,\varepsilon} \approx -\frac{1}{V}\left(\frac{\Delta V}{\Delta P}\right)_{T,\varepsilon}.$$

Thus for the "rubbery" state under 500K, the isothermal compressibility was determined as $\kappa_{500K} = 2.98 \times 10^{-4} atm^{-1}$ while in the moderate cooling process $\kappa_{300K} = 1.02 \times 10^{-4} atm^{-1}$. These are both significant at the 1% level.

ACKNOWLEDGEMENT

We sincerely give thanks to Prof. Lonnie Crosby for his mentorship and Prof. Kwai Wong for his support throughout this project. This work was also funded by National Science Foundation (NSF) and largely supported by Joint Institute for Computational Science (JICS), University of Tennessee (UT) and Oak Ridge National Laboratory (ORNL) for all facilities and computational resources.

[1] F.-L. Jin, X. Li, and S.-J. Park, Journal of Industrial and Engineering Chemistry **29**, 1 (2015).
[2] C. Wu and W. Xu, Polymer **47**, 6004 (2006).
[3] V. Varshney, S. S. Patnaik, A. K. Roy, and B. L. Farmer, Macromolecules **41**, 6837 (2008), http://dx.doi.org/10.1021/ma801153e.
[4] J. Choi, S. Yu, S. Yang, and M. Cho, Polymer **52**, 5197 (2011).
[5] H. B. Fan and M. M. Yuen, Polymer **48**, 2174 (2007).
[6] Z. Wang, Q. Lv, S. Chen, C. Li, S. Sun, and S. Hu, Molecular Simulation **41**, 1515 (2015), http://dx.doi.org/10.1080/08927022.2014.998213.
[7] C. Wu and W. Xu, Polymer **48**, 5802 (2007).
[8] K. Vanommeslaeghe, E. Hatcher, C. Acharya, S. Kundu, S. Zhong, J. Shim, E. Darian, O. Guvench, P. Lopes, I. Vorobyov, and A. D. Mackerell, Journal of Computational Chemistry **31**, 671 (2010).
[9] W. Yu, X. He, K. Vanommeslaeghe, and A. D. MacKerell, Journal of Computational Chemistry **33**, 2451 (2012).
[10] K. Vanommeslaeghe and A. D. MacKerell, Journal of Chemical Information and Modeling **52**, 3144 (2012), pMID: 23146088, http://dx.doi.org/10.1021/ci300363c.
[11] K. Vanommeslaeghe, E. P. Raman, and A. D. MacKerell, Journal of Chemical Information and Modeling **52**, 3155 (2012), pMID: 23145473, http://dx.doi.org/10.1021/ci3003649.
[12] C. G. Mayne, J. Saam, K. Schulten, E. Tajkhorshid, and J. C. Gumbart, Journal of Computational Chemistry **34**, 2757 (2013).
[13] G. A. Petersson, A. Bennett, T. G. Tensfeldt, M. A. Al-Laham, W. A. Shirley, and J. Mantzaris, The Journal of Chemical Physics **89**, 2193 (1988), http://dx.doi.org/10.1063/1.455064.
[14] G. A. Petersson and M. A. Al-Laham, The Journal of Chemical Physics **94**, 6081 (1991), http://dx.doi.org/10.1063/1.460447.
[15] A. D. Becke, The Journal of Chemical Physics **98**, 5648 (1993), http://dx.doi.org/10.1063/1.464913.
[16] M. Valiev, E. Bylaska, N. Govind, K. Kowalski, T. Straatsma, H. V. Dam, D. Wang, J. Nieplocha, E. Apra, T. Windus, and W. de Jong, Computer Physics Communications **181**, 1477 (2010).
[17] L. Martínez, R. Andrade, E. G. Birgin, and J. M. Martínez, Journal of Computational Chemistry **30**, 2157 (2009).
[18] J. M. Martínez and L. Martínez, Journal of Computational Chemistry **24**, 819 (2003).